

Peculiarities of interaction of gold nanoparticles with photoinitiators in polymer nanocomposites for holographic recording

J. Burunkova¹, M.-J. Ohoueu², I. Csarnovics³, M. Veres⁴, A. Bonyár⁵, S. Kokenyesi³

¹ITMO University, Saint-Petersburg, Russia

²New Mexico Highlands University, New Mexico, USA

³Institute of Physics, University of Debrecen, Debrecen, Hungary

⁴Wigner Research Centre for Physics, Hungarian Academy of Sciences, Budapest, Hungary

⁵Department of Electronics Technology, Budapest University of Technology and Economics, Budapest, Hungary

Abstract:

The influence of gold nanoparticles (AuNPs) on the decomposition of two widely used types of photoinitiators (Bis (.eta.5-2,4-cylcopentadien-1-yl)-bis (2,6-difluoro-3-(1H-pyrrol-1-yl)-phenyl) titanium /Irg784/ and 2,2-Dimethoxy-2-phenylacetophenone /In2/) was investigated in this work, both, in simple toluene solutions or solutions with AuNPs, as well as in SiO₂ nanoparticles and AuNPs containing monomer acrylate nanocomposites during photopolymerization. These processes are important for efficient, one-step creation of photonic structures by holographic recording based on polymer nanocomposites containing AuNPs with plasmonic properties.

Analysing such processes, activated by irradiation with wavelengths of 532 nm and 325 nm, their efficiency and parameters of grating recording, as well as examining the related multistep photopolymerization processes by IR and UV-VIS spectroscopy the influence of AuNPs on the decomposition of the photoinitiators was shown and explained by the mechanism of complex formation. Thereby, it is concluded that by combining the type of initiator, polymer matrix components, and illumination conditions the decomposition of

initiators can be manipulated, that in turn affect the resulting optical modulation characteristics and the efficiency of the photonic elements recording in a one-step process.

Keywords: Photopolymerization; polymer nanocomposites; Photoinitiator Bis (4,5-2,4-cyclopentadien-1-yl)-bis (2,6-difluoro-3-(1H-pyrrol-1-yl)-phenyl) titanium; Photoinitiator 2,2-Dimethoxy-2-phenylacetophenone; gold nanoparticles; decomposition of photoinitiator, optical recording process; holographic recording.

*Corresponding author: e-mail – csarnovics.istvan@science.unideb.hu, phone - +36-70-331-4744.

1. Introduction

Photo-curable nanocomposite materials are mixtures of monomers and organic or inorganic compounds, and they serve as the basis for the development of smart materials for electronics, photonics, etc. [1,2]. A wide number of polymer nanocomposites with different inorganic and organic nanoparticles was investigated and developed for hologram recording by Y.Tomita with co-authors [3-8]. The redistribution of neutral components plays an essential role in the recording processes, as described in [9] as well. Blending gold nanoparticles (AuNPs) with photocurable materials gives new abilities at the stage of photo-sensitive element fabrication or new functionalities in devices based on these materials and elements. These effects can be extended to other applications of AuNPs in composites, where the electronic, optical and plasmonic effects determine new functionalities in photonics, optoelectronics, catalysis, and bioengineering [10-15]. Yang Tian and Tetsu Tatsuma reported the visible light induced plasmon resonance in AuNPs which resulted in charge separation and redox reactions [16, 17]. This makes AuNPs potentially useful as photocatalysts, elements of photovoltaic fuel cells, and for optical patterning as well. Fox et al. studied properties of *trans*-stilbene- and *o*-nitrobenzyl-ether-functionalized AuNPs [18], while Kamat and Thomas investigated intramolecular energy and electron-transfer reactions in fullerene- and pyrene-functionalized AuNPs [19]. These experiments demonstrated that AuNPs could be used as electron acceptors or modifiers of light-stimulated processes in different matrixes, and these modifications may depend on the type of functionalization of AuNPs as well. Nakashima and Nonoguchi first reported the use of a semiconductor nanocrystal as donor-acceptor electron transfer initiator in the presence of an onium salt for radical photopolymerization of an ionic

liquid-based acrylic monomer [20]. The radical photopolymerization of an acrylic monomer with 5-mercapto-2,2'-bithiophene functionalized AuNPs using [4-[(acetyloxy)phenyl] phenyl] iodonium hexafluoroantimonate as a co-initiator and respectively without the use of conventional photoinitiators has been described in [21, 22]. For this reason and possible peculiar applications, photo-curable polymer composites containing AuNPs are worthy of serious attention in research and development. For example, nowadays photonic crystal (PhC) structures (including ones with localized surface plasmon resonance effect) are among the main objects of scientific research and application of nanotechnology in photonics, sensors [23, 24]. There are various well-known multistep methods to produce PhC using different materials. Mostly they are formed as 1D and 2D structures, while only a few of them allow the fabrication of 3D ones. One of the possible ways to produce them is the multibeam interference holographic recording method using polymer nanocomposites on the basis of different monomers and inorganic nanoparticles [25-28]. Here the processes of photostimulated polymerization of monomers and associated diffusion of nanoparticles and monomers are responsible for the creation of photonic structures by holographic recording in the selected nanocomposite. These polymer nanocomposites allow the direct, single-step creation of PhC with localized surface plasmon resonance effect too. In last few years our group produced polymer nanocomposites with AuNPs for holographic recording of photonic crystal structures [27-29]. A nanocomposite containing Er and Yr nanoparticles besides AuNPs was developed and it was shown [25] that as a result of the metallic nanoparticles addition the luminescence was enhanced 8-times.

It was observed in these works that AuNPs affect on the recording process depending on the monomer compositions, type of the photoinitiator and irradiation parameters. They influence the rate and magnitude of conversion in the photopolymerization processes and so the surface magnitude of resulting PhC structures, wherein the localized surface plasmon resonance of AuNPs remains unchanged after recording such structures and may be active in sensing applications of such PhCs. However, the influence of AuNPs on the processes occurring during polymerization of nanocomposites, especially the mechanism of such effects, has not been identified yet. Since polymerization is a multistep process and each stage can be affected by the AuNPs, the detailed analysis and understanding of the possible effects are quite important. To the best of our knowledge, there are no works discussing the influence of AuNPs on the decomposition of photoinitiators during the photopolymerization process.

In this paper, we investigate in details the influence of AuNPs on the process of photopolymerization in polymer nanocomposites, highlighting their influence on photoinitiators, their decomposition and so on the resulting efficiency of optical recording, as it was observed earlier in our paper [25-28]. The results of our study may be useful for further development and applications of light-sensitive polymer nanocomposites, combining their parameters for direct, one-step fabrication of different photonic elements.

2. Experimental methods

2.1. Materials for the preparation of the polymer nanocomposites.

The following monomers, nanoparticles, and photoinitiators were used for the investigation:

- Diurethane dimethacrylate (No. 436909, Aldrich, UDMA)
- Isodecyl acrylate (No. 408956 Aldrich, IDA),
- Dodecanethiol functionalized AuNPs (No. 3014, Nanoprobes, Au-SCH₂(CH₂)₁₀CH₃,
Size concerning TEM measurement – 5 nm),
- SiO₂ nanoparticles (Aldrich S5130– Silica NPs powder, size concerning TEM
measurement - 7 nm)
- 2,2-Dimethoxy-2-phenylacetophenone ,No. 19611-8 Aldrich (In2). Chemical formula
C₁₆H₁₆O₃, see the chemical structure in Figure 4.
- Bis(.eta.5-2,4-cylcopentadien-1-yl)-bis(2,6-difluoro-3-(1H-pyrrol-1-yl)-phenyl)
titanium (Irg784). Chemical formula C₃0H₂2F₄N₂Ti, see the chemical structure in
Figure 4.

The resulting nanoparticles and nanocomposites were characterized by TEM
(Transmission Electron Microscope) JEOL-2000FXII (see Figure 1.b).

2.2. Preparation of the solutions

A certain amount of initiator corresponding to the desired weight percent in the
nanocomposite (see data in Table 1) was dissolved in toluene. For the preparation of the AuNPs containing a mixture, a calculated amount of AuNPs solution, having a concentration of 0.0032 g/ml in toluene was added to the initiator solution. In the case of the Irg784

solution, the weighted compound was initially dissolved in dichloromethane prior to the addition of toluene. To investigate the influence of the AuNPs, a solution with a different amount of compounds was created (see Table 1). To change the ratio of photoinitiator/ AuNPs the amount of used photoinitiator was different, while the amount of AuNPs was the same. The exact composition of the solutions is presented in Table 1. Solutions are labeled by S, nanocomposites - by P, and the type of initiators, the presence of AuNPs are shown additionally.

Symbol of the solution	The composition of the solution	Amount of compounds in solution	The ratio of Photoinitiator/AuNPs
SAu	AuNPs/Toluene	0.3 mg/4.9 ml AuNPs – 0.0077 wt%	-
SIrg	Irg784/Toluene	1.5 mg/6.07 ml Irg784 - 0.0277 wt%	-
SIrgAu1	AuNPs/Irg784/Toluene	0.4 mg/2.9 mg/6.07 ml AuNPs - 0.0077 wt% Irg784 - 0.0555% wt%	7.21
SIrgAu2	AuNPs/Irg784/Toluene	0.4 mg/1.5 mg/6.07 ml AuNPs - 0.0077 wt% Irg784 - 0.0277 wt%	3.59
SIn	In2/Toluene	1.0 mg/ 5ml In2 - 0.02325 wt%	-
SInAu1	AuNPs/In2/Toluene	0.3 mg/2.0 mg/5 ml AuNPs - 0.0069 wt% In2 - 0.0511 wt%	7.41
SInAu2	AuNPs/In2/Toluene	0.3 mg/1.1 mg/5 ml AuNPs - 0.0069 wt% In2 - 0.0256 wt%	3.71

Table 1: Details of the created solutions.

2.3. Preparation of the nanocomposites

Two types of nanocomposites were created and studied: systems with and without AuNPs. The mixture of monomer materials (UDMA and IDA) was stirred together for 3 h. In the next

stage, SiO₂NPs were added step by step to the prepared monomer mixture. Magnetic stirring was applied to prepare the nanocomposites during 24 h. After this step, the solution of AuNPs in toluene was added to the above-mentioned mixture of monomers and was stirred for 24 hours again. Finally, photoinitiator was added and the prepared nanocomposites were stirred for another 3 h.

To investigate the influence of the AuNPs, nanocomposites with different amount of compounds was created. The ratio of photoinitiator/AuNPs was changed, for this the amount of AuNPs was different, while the amount of photoinitiator was the same. The prepared nanocomposites are listed in Table 2.

Symbol of the composition	Monomer composition	SiO ₂ NPs [wt% of sum of monomers]	AuNPs [wt% of sum of monomers and SiO ₂ NP]	Photoinitiator [wt% of sum of monomers]	Ratio of photoinitiator/AuNPs
PAu	UDMA/IDA=7/3 (7g/3g)	10 (1,1g)	0.15 (0,0167g)	-	-
PIrg	UDMA/IDA=7/3 (7g/3g)	10 (1,1g)	-	0.5 (Irg784) (0,05g)	-
PIrgAu1	UDMA/IDA=7/3 (7g/3g)	10 (1,1g)	0.08 (0,0089g)	0.5 (Irg784) (0,05g)	6.25
PIrgAu2	UDMA/IDA=7/3 (7g/3g)	10 (1,1g)	0.15 (0,0167g)	0.5 (Irg784) (0,05g)	3.33
PIn	UDMA/IDA=7/3 (7g/3g)	10 (1,1g)	-	0.5 (In2) (0,05g)	-
PInAu1	UDMA/IDA=7/3 (7g/3g)	10 (1,1g)	0.08 (0,0089g)	0.5 (In2) (0,05g)	6.25
PInAu2	UDMA/IDA=7/3 (7g/3g)	10 (1,1g)	0.15 (0,0167g)	0.5 (In2)	3.33

Table 2: List and amount of components in the prepared nanocomposites.

Film samples were prepared in a next way: the droplet of monomer nanocomposite was placed on a glass substrate and covered with mylar film to prevent contact with atmosphere oxygen, which inhibits the polymerization. Thin film thickness usually was set by 55 μm spacer between the substrate and cover film. Hard films, holographic structures were obtained by proper irradiation of such samples. Optical measurements were done in cuvettes (liquids) or on a thicker (300 μm spacer) liquid sample structures or solid polymer films.

2.4. Measurements of decomposition of photoinitiators and investigation of the recorded structures.

To investigate the illumination-induced processes, the prepared solutions and nanocomposites were irradiated with light emitting diodes (MPL-F-355nm) through a filter being transparent at 325 nm or with a green laser setup (PGL-V-II-532 nm). Both light sources were defocused, so the power density delivered to the sample was 4 mW/cm². The changes of parameters of solutions under illumination were measured in quartz glass cuvettes, while the nanocomposites were placed between quartz glass plates with 300 μm spacers for the irradiation, optical measurements and with 55 nm spacers for holographic recording. The whole surface area of the tested samples, solutions, and nanocomposites was irradiated.

Holographic recording, i.e. recording the interference pattern of two coherent laser beams, was performed at proper light wavelengths and resulted in gratings with period 2 μm with phase (thickness and refractive index) modulation. The efficiency of recording (which consists of polymerization processes combined with mass-transport of monomers and nanoparticles) was determined as the diffraction efficiency of the recorded phase grating, i.e. as the ratio of the light intensity diffracted to the first diffraction peak and the incident readout light intensity [22]. The 2D and 3D images of the created PhC, their cross-section, period and average modulation depth were measured by atomic force microscope (AFM - Veeco diCaliber). In parallel, some direct measurements of periodical surface relief depth were made by AFM on a free surface of polymer grating sample after the recording. It gave us an information about the amplitude of the created surface structures (see Figure 1.a).

Spectral data were recorded with a UV-VIS spectrophotometer (UV-1800 SHIMADZU) and infrared (IR) spectrophotometer (Bruker TENSOR37). The kinetics of Irg784 and In2 photoinitiators dissociation upon light irradiation was determined by measuring the decrease of the absorption peaks at 470 nm and 340 nm, respectively, which are characteristic for these materials. The rate of initiators decomposition due to the irradiation was measured as the

initial slope of the curve, which describes the decrease of the initiator's absorption with irradiation time: for In2 this is the peak at 340 nm, for Irg784 – at 470 nm.

3. Results and Discussion

It was shown in our previous work that AuNPs can be added successfully to polymer nanocomposites and photonic crystals (PhC) can be created via two-beam interference recording [20,21], as well as by multibeam recording [22]. Now in one case in one case In2, photoinitiator (nanocomposites PIn and PInAu absorbing light only in the UV region, without significant absorbance at the plasmon peak of AuNPs) was chosen to produce a simple PhC in the form of volume grating. These PhCs were recorded by irradiation with a light source working at 325 nm. However, in many cases, it is easier to use a light source which is emitting in the visible region – blue or green. So for this case, an Irg784 photoinitiator (which is sensitive up to 550 nm, nanocomposites PIrg, and PIrgAu1-2) was chosen to produce PhCs. These were recorded by irradiation with a light source working at 532 nm. For both nanocomposites containing AuNPs (PInAu1-2 and PIrgAu1-2) the resonant plasmon absorption peak of the AuNPs was established at 530 nm and its position and form change not noticeable after irradiation of solutions, recording the spatially modulated (phase and thickness) PhC structure. It means that AuNPs are single embedded in the matrix, as shown in Figure 1.b.

The compositions of the investigated polymer nanocomposites differ in the type of the photoinitiator only. However, the change of both the photoinitiator and irradiation wavelength led to different results (see Table 3).

Symbol of the nanocomposite sample	The amplitude of the created surface structure [nm]	Diffraction efficiency [%]
PIrg	200	6
PIrgAu2	100	2
PIn	20	10
PInAu2	38	25

Table 3: Details of the holographic recording in different polymer nanocomposites.

It was shown that the addition of AuNPs reduced the modulation amplitude and the diffraction efficiency of the created PhCs for nanocomposites PIrg-PIrgAu (containing

photoinitiator Irg784). While in nanocomposites PIn-PInAu (containing photoinitiator In2) AuNPs enhanced these parameters. The process of holographic recording is connected with the photopolymerization, where the decomposition of the photoinitiator is the first step, so it is important to investigate the influence of AuNPs on this process in order to understand better the whole mechanism of it. For this reason, we investigated the influence of AuNPs on the decomposition of photoinitiators in different media (solution and nanocomposite). As it will be shown later, the localized plasmon resonance of the selected AuNPs is close to 530 nm, so two types of initiators which were chosen (In2 and Irg784, not absorbing and absorbing light at 530 nm, respectively) allow us investigate the mechanism of decomposition of the photoinitiators upon irradiation within or outside the spectral range of plasmon resonance of AuNPs.

Samples with toluene solutions can be treated as model systems since there are no monomers, and the possible direct interaction of photoinitiators and AuNPs can be investigated. Absorption spectra and kinetics of photoinitiator decomposition were studied first in such solutions during the irradiation process. The peak of localized plasmon resonance of the added AuNPs was determined in toluene solutions and in nanocomposites without photoinitiators. It was found to be at 530 nm (Figure 1.a, curve 3 and Figure 2.a, curve 3). Stability of the AuNPs absorption spectra was observed during irradiation of the AuNPs containing solution as well as AuNPs containing nanocomposites without photoinitiators using 325 nm and 532 nm light. The position and shape of the peak were not changed noticeably in both studied systems.

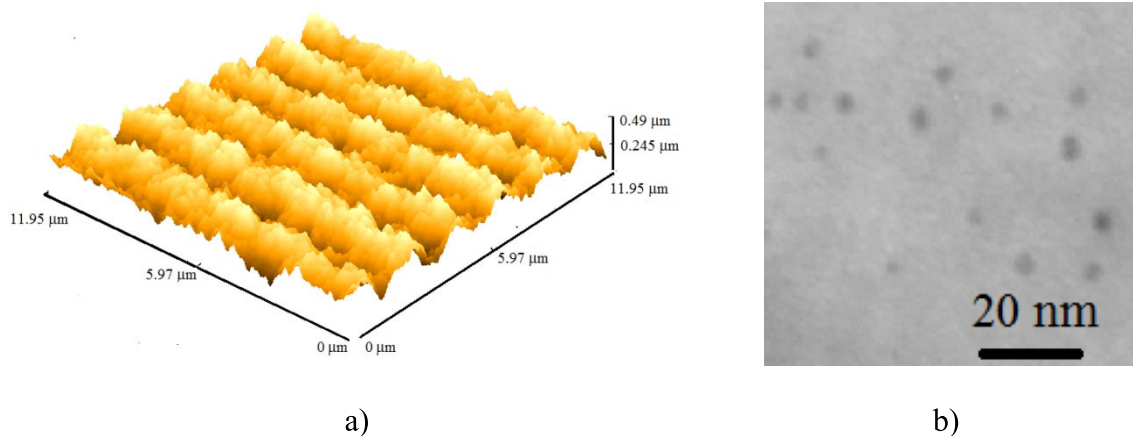


Figure 1. a) AFM picture of a free surface of polymer grating sample after the recording, b) TEM picture of AuNPs in UDMA/IDA nanocomposite.

3.1. Investigation of the influence of AuNPs on the Irg784 photoinitiator decomposition during irradiation by 532 nm

Decomposition of photoinitiator was studied in solution for Irg784 due to irradiation of SIrg, SIrgAu1 and for SIrgAu2 by measuring the absorption at 470 nm. It was shown that the absorption of this peak decreased for both solutions, see Fig. 2.a and b. The rate of initiators decomposition due to the irradiation was measured as the initial slope of the curves in Fig. 2.c. It could be seen in this figure, that the ratio of photoinitiator/AuNPs has an influence on the decomposition rate of photoinitiator. Adding AuNPs and decreasing the mentioned ratio results in the decrease of decomposition rate. So the presence of AuNPs and their ratio to Irg784 in toluene affect on the studied process, reducing the decomposition rate of this photoinitiator.

Besides of it, the addition of the photoinitiator Irg784 to SAu solution resulted in a 45 nm red shift of the plasmon peak of AuNPs (Figure 2.b, compared curve 3 and 4: the shift is clearly observable). After the irradiation of this solutions by 532 nm light, the resonance peak of AuNPs has further shifted to higher wavelength totally 60 nm in comparison with SAu (Figure 2.b, compared curve 3 and 5: the shift is clearly observable).

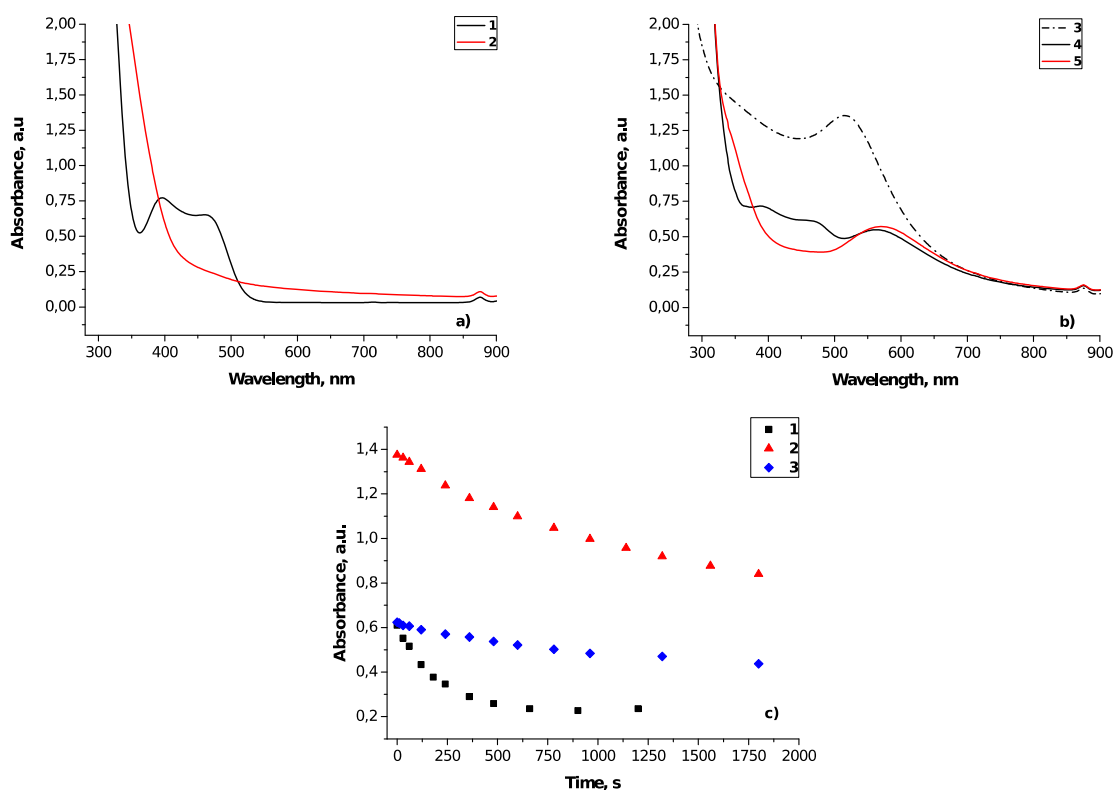


Figure 2. (a) Absorbance spectra of the investigated solutions before (bef) and after (aft) irradiation by green laser setup (532 nm) with and without AuNPs: 1 – SIrg bef; 2 – SIrg aft;

- (b) Absorbance spectra of the investigated solutions before (bef) and after (aft) irradiation by green laser setup (532 nm) with and without AuNPs: 3 – SAu; 4 – SIrgAu2 bef; 5 – SIrgAu2 aft.
- (c) Effect of AuNPs on the kinetics of Irg784 decomposition in toluene: 1 – SIrg, 2 – SIrgAu1, 3 – SIrgAu2.

An acrylate monomer mixture (Table 2) was used to study the effect of AuNPs on the decomposition rate of photoinitiator Irg784 during irradiation at 532 nm. This wavelength coincides with the spectral range of plasmon resonance of the AuNPs used in our experiments. The absorption spectra of the PIrg and the PIrgAu2 nanocomposites measured at different stages of the irradiation are provided in [Figure 3.a, b, and c](#).

Decomposition of photoinitiator was studied in composition for PIrg and for PIrgAu samples as well by measuring the absorption at 470 nm due to irradiation. It was shown that the absorption of this peak decreased for both nanocomposites, see [Fig. 3.a and b](#). The rate of initiators decomposition due to the irradiation was measured as the initial slope of the curves in [Fig. 3.c](#). The decomposition rates for PIrg and PIrgAu2 during irradiation are demonstrated in [Figure 3.c](#). It can be seen in that the presence of AuNPs increased the decomposition rate of the Irg784 in acrylate nanocomposites. Besides, it was we established, as it follows from [Fig. 3.c](#), curve 2 and 3 that increasing the concentration of AuNPs in the composition leads to significantly enhanced Irg784 decomposition rate in acrylate nanocomposites. So the presence of AuNPs in nanocomposites at the given concentration enhanced the decomposition of this photoinitiator.

Besides of it, the addition of the photoinitiator Irg784 to PAu nanocomposites resulted in an 80-110 nm red shift of the plasmon peak of AuNPs ([Figure 3.b](#), compared curve 3 and 4: the shift is clearly observable). After the irradiation of this solutions by 532 nm light, the resonance peak of AuNPs has further shifted to higher wavelength in comparison with PAu ([Figure 3.b](#), compared curve 3 and 5: the shift is clearly observable).

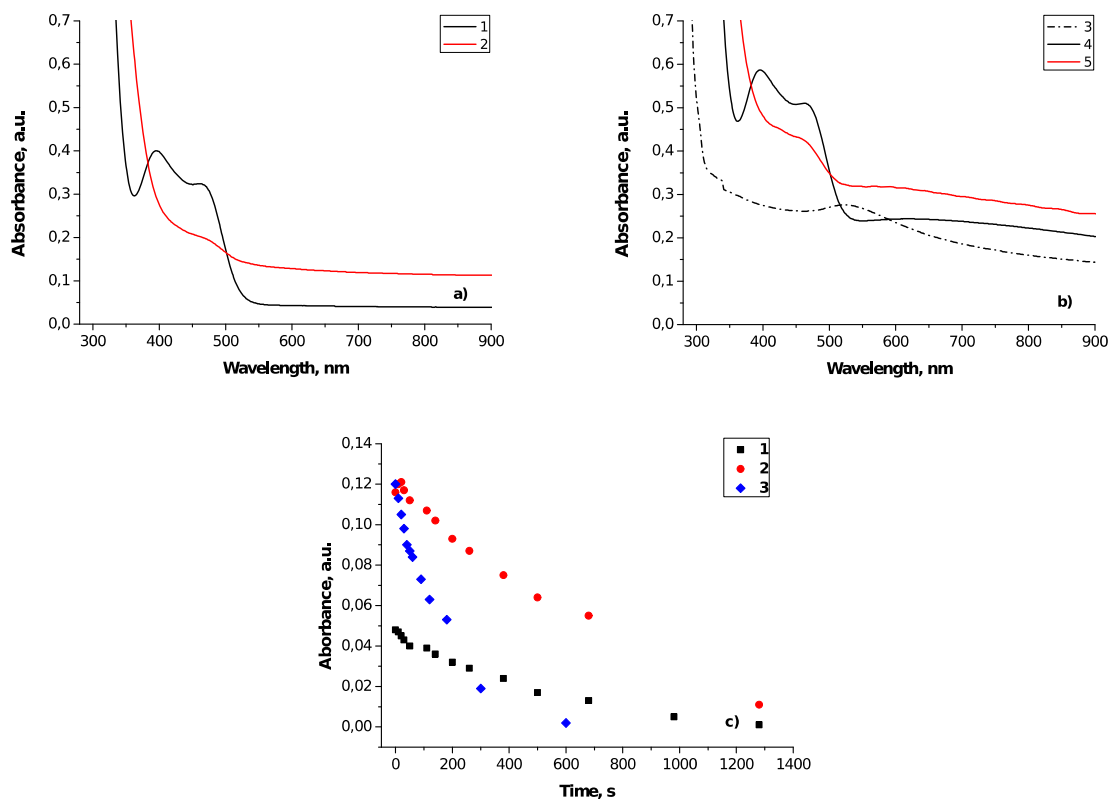


Figure 3. a) Absorption spectra of acrylate nanocomposites before (bef) and after (aft) irradiation by 532 nm: 1 – PIrg bef; 2 – PIrg aft;
 b) Absorption spectra of acrylate nanocomposites before (bef) and after (aft) irradiation by 532 nm: 3 – PAu; 4 – PIrgAu2 bef; 5 – PIrgAu2 aft.
 c) Kinetics of Irg784 decomposition in acrylate nanocomposites during irradiation at 532 nm: 1 – PIrg; 2 – PIrgAu2, 3 – PIrgAu2

Thus, after analyzing the absorption spectra and the decomposition kinetics of Irg784 in solution and in the nanocomposites at irradiation by 532 nm light, the following effects can be noted: no changes in Irg784 absorption peak positions; a significant shift of the AuNPs plasmon peak towards higher wavelengths in SIrgAu and PIrgAu medias; the addition of AuNPs reduced the Irg784 decomposition rate in the solution and increased it in the nanocomposite; this rate depends on the ratio of photoinitiator/AuNPs (decrease of this ratio leads to larger influence).

It can be seen that AuNPs affect the decomposition of Irg784 photoinitiator in the solution and in the nanocomposites differently. Based on these data, the formation of an AuNPs - Irg784 complex may be assumed. This is in good agreement with other observations on Irgacure decomposition [30] stating that the intensity of the electromagnetic field – affected by the plasmonic AuNPs in our system – has strong effect on the decomposition mechanism

of the photoinitiator, which may be the reason behind the complex formation as well. The latter may occur through formation of a donor-acceptor bond between the phenyl or pyrrole rings of the initiator and the positively charged surface of the AuNPs, known as acceptors of negatively charged particles. Structures of Irg784 and In2 photoinitiators as well as the products of their photo-dissociation are presented in Fig.4.

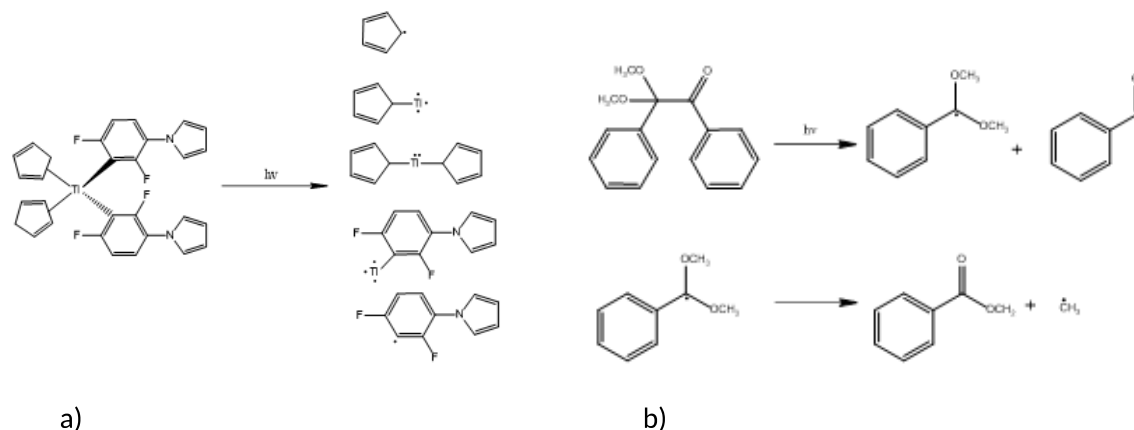


Figure 4. The molecular structure and the products of photo-dissociation of the photoinitiators under UV irradiation: a) Irg784 [31,32] and b) In2 [33]

In order to study the complex formation between the photoinitiator and the AuNPs FTIR spectra of dry residues of SIrg and SIrgAu2 were measured before and after the 532 nm irradiation (Figure 5).

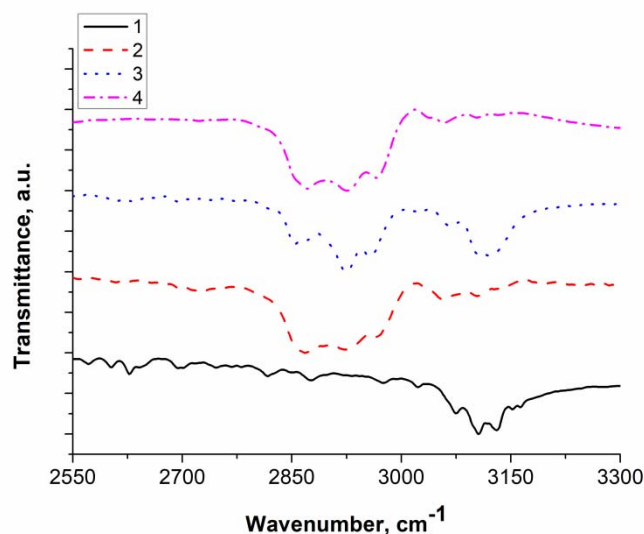


Figure 5. FTIR spectra before (bef) and after (aft) irradiation of the dry residue of SIrg and SIrgAu2: 1 – SIrg bef; 2 – SIrg aft; 3 – SIrgAu2 bef; 4 – SIrgAu2 aft.

The comparison of the FTIR spectra of the dry residues of pure SIrg and SIrgAu2 shows that the presence of nanoparticles affects the structure of the photoinitiator and decomposition

products. Noticeable changes can be seen in the CH stretching region, where the peaks of aromatic CH stretch above 3000 cm^{-1} broaden and overlap. In this region bands in the $3020\text{--}3130\text{ cm}^{-1}$ region correspond to the stretching vibrations of C–H bonds in aromatic compounds. 2850 , 2870 , 2925 and 2955 cm^{-1} peaks can be attributed to symmetrical (sym) and asymmetrical (assym) vibrations of sp^3CH_2 sym, sp^3CH_3 sym, sp^3CH_2 assym, and sp^3CH_3 assym, respectively [34]. So the above changes mean that the insertion of AuNPs effects bands corresponding to the vibrations of the aromatic ring.

After the irradiation, the vibration bands corresponding to the aromatic structure were preserved in the samples with AuNPs but were shifted and their intensity ratios changed. The shape of the spectra of the reaction products after the irradiation is almost the same for both SIrg and for SIrgAu2 samples. The intensity of the band at 3100 cm^{-1} strongly decreases after the 532 nm irradiation for SIrg and for SIrgAu2 as well, indicating remarkable changes in the bonding configuration of the aromatic rings. In the spectra of SIrgAu2, the intensity of the sp^3CH_3 bands decreases after irradiation. This means that there are less CH_3 terminal groups and more sp^3CH_2 or sp^3CH cross-linked groups in the reaction products of Irg784 with AuNPs. The bands at 2850 , 2870 , 2925 , and 2955 cm^{-1} are preserved for SIrgAu2 after irradiation, but their intensity ratio is changed. The band at 2955 cm^{-1} is shifted to 2960 cm^{-1} indicating the presence of sp^2CH_2 sym vibrations. Moreover, a sp^2CH_2 asym vibrational peak appears at 3070 cm^{-1} . These sp^2CH_2 vibrations arise not from the benzene ring, but from the C-H vibrations of $\text{H}_2\text{C}=\text{C-R}$ group. All the analyzed effects testify that interaction of AuNPs with Irg784 occurs.

The molar concentrations of AuNPs are three orders of magnitude lower than of the initiators. Therefore, only a part of the initiator molecules may form complexes with AuNPs, while several of them will remain unchanged. This fact explains the remarkable shift of the AuNPs peak in the solution (Figure 2.b) compared to the weak shift of the Irg784 initiator peak. It is important to mention, that the selected concentration of gold nanoparticles in composites is sufficient to make the average distance between them not more as 100 nm if uniformly distributed.

In the toluene solution, the formation of AuNPs - Irg784 complex leads to the increased stability of initiator to the irradiation by 532 nm , which is expressed in the reduced decomposition rate. In the given example of concentrations in acrylate matrix, the AuNPs influenced the decomposition rate of Irg784 in another way. There we see the different effect, what may be caused by the increased concentration of non-complexed Irg 784, which undergo

decomposition under the influence of excited plasmon fields of AuNPs. The possible differences in thermal effects due to the radiation absorption- heat dissipation in AuNP surroundings on Irg 784 decomposition may be also supposed, but these need separate investigations with different concentration of interacting components.

3.2 Investigation of the influence of AuNPs on the In2 photoinitiator decomposition during irradiation by 325 nm

Decomposition of In2 photoinitiator was studied in solution SIn and SInAu2 as well by measuring the absorption at 340 nm due to irradiation. It was shown that the absorption of this In2 peak decreased for both solutions, see Fig. 6.a and b. The rate of initiators decomposition due to the irradiation was measured as the initial slope of the curves in Fig. 6.c. The decomposition rates for SIn, SInAu1, and SInAu2 during irradiation are demonstrated in Fig. 6.c. It can be seen that the AuNPs decreased the decomposition rate of the photoinitiator. Moreover, the lower the ratio of photoinitiator/AuNPs, greater the influence, so adding AuNPs to In2/Tol solution slows down the decomposition rate of the photoinitiator. Twice higher amount of AuNPs in comparison to In2 led to a decreased decomposition rate (Figure 6.c, curve 3). So the presence of AuNPs in toluene at the given concentration reduced the decomposition of this photoinitiator.

In addition, the presence of the In2 (Figure 6.b) has no any influence on the position of the 530 nm AuNPs peak. After 325 nm irradiation and decomposition of the In2, the AuNPs peak shifted to the higher wavelength region with 20–40 nm (Figure 6.b, compared curve 3, 4 and 5: the shift is clearly observable).

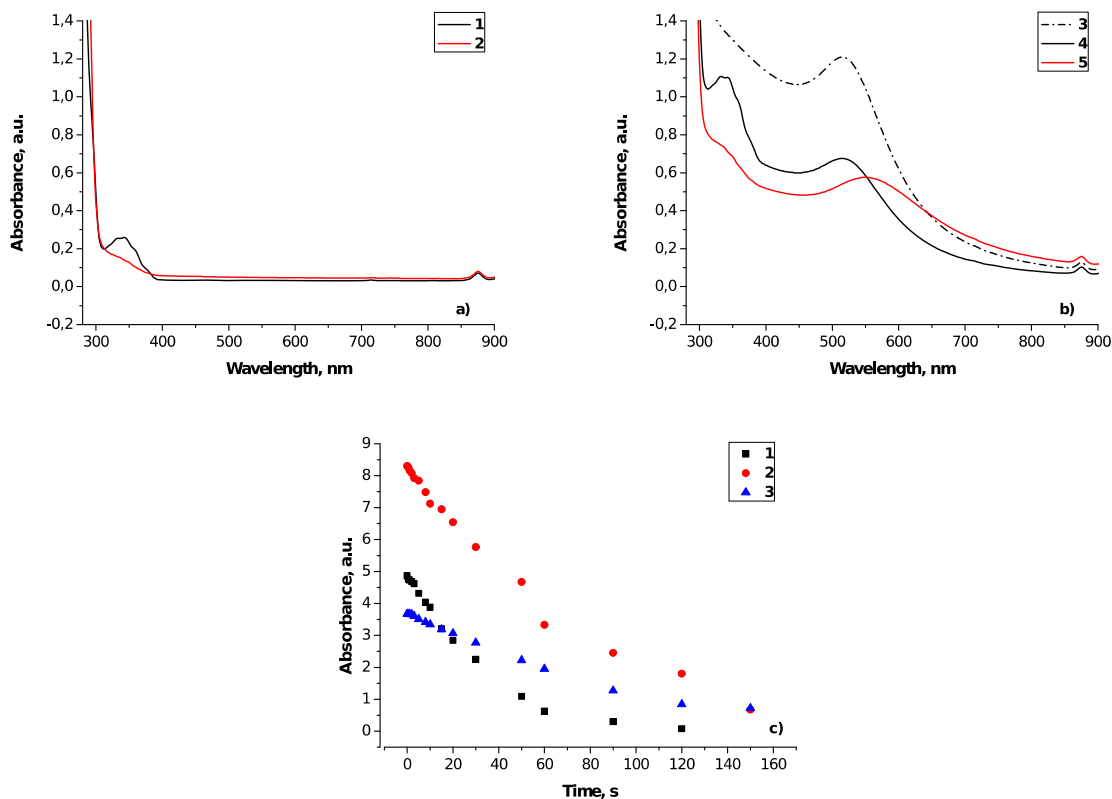


Figure 6. (a) Absorbance spectra of the investigated solutions before (bef) and after (aft) irradiation by 325 nm with and without AuNPs: 1 – SIn bef; 2 – SIn aft; (b) Absorbance spectra of the investigated solutions before (bef) and after (aft) irradiation by 325 nm with and without AuNPs: 3 – SAu; 4 – SInAu2 bef; 5 – SInAu2 aft. (c) Effect of AuNPs on the kinetics of In2 decomposition in toluene: 1 – SIn; 2 – SInAu1; 3 – SInAu2.

An acrylate monomer mixture (Table 2) was used to study the effect of AuNPs on the decomposition rate of photoinitiator In2 during irradiation at 325 nm. The absorption spectra of the PIn and the PInAu2 measured at different stages of the irradiation are provided in Figure 7.a, b, and c.

Decomposition of photoinitiator was studied in nanocomposites for PIn and for PInAu2 samples as well by measuring the absorption at 340 nm due to irradiation. It was shown that the absorption of this peak decreased for both nanocomposites, see Fig. 6.a and b. The rate of initiator decomposition due to the irradiation was measured as the initial slope of the curves in Fig. 7.c. The decomposition rates for PIn, PInAu1, and PInAu2 during irradiation are demonstrated in Figure 7.c. In addition, the presence of AuNPs in the nanocomposites results in the decrease of the photoinitiator decay rate during irradiation (Figure 7.b). This effect is

more emphasized for higher AuNPs concentrations. It can be seen in that the presence of AuNPs decreased the decomposition rate of the In2 in acrylate nanocomposites.

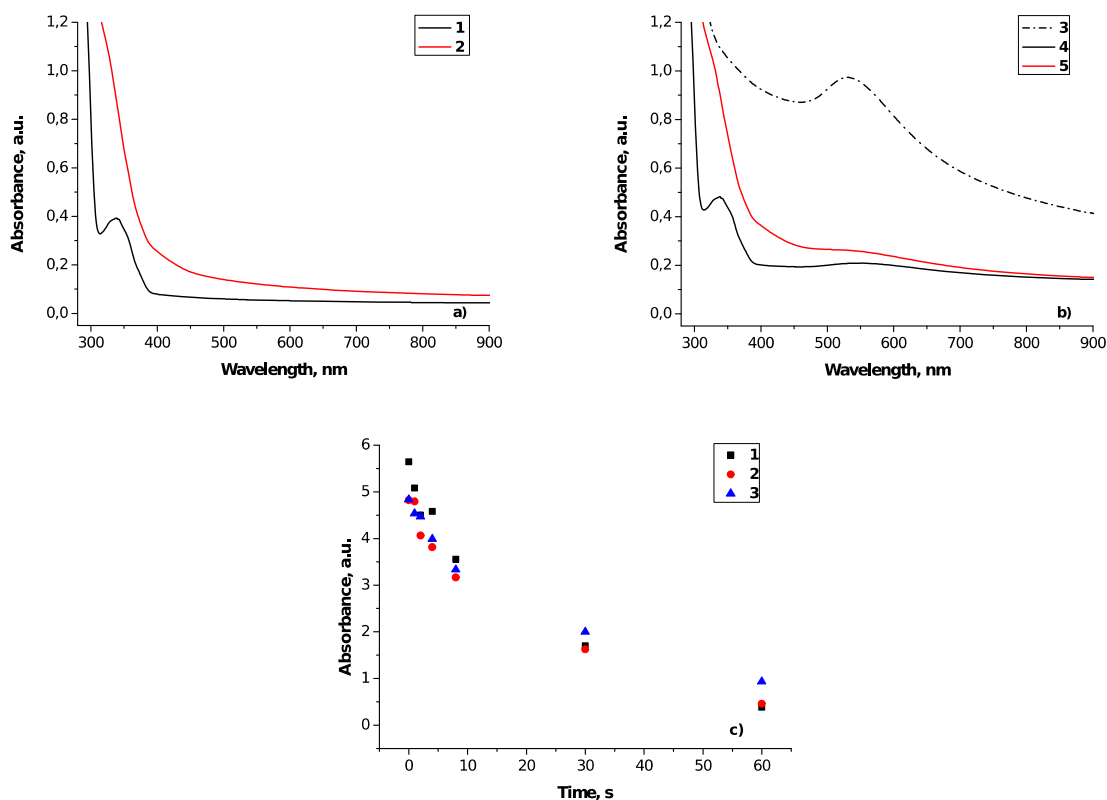


Figure 7. a) Absorption spectra of acrylate nanocomposites before (bef) and after (aft) irradiation by 325 nm: 1 – PIn bef; 2 – PIn aft;
b) Absorption spectra of acrylate nanocomposites before (bef) and after (aft) irradiation by 325 nm: 3 – PAu; 4 – PInAu2 bef; 5 – PInAu2 aft.
c) Kinetics of In2 decomposition in acrylate nanocomposites during irradiation by 325 nm: 1 – PIn; 2 – PInAu1; 3 – PInAu2.

Thus, after analyzing the absorption spectra and In2 decomposition kinetics in solution and nanocomposites at irradiation by 325 nm light, the following effects can be noted: there is no significant shift of In2 peak positions; the presence of photoinitiator has no influence on the plasmon peak position of AuNPs; the addition of AuNPs has reduced the decomposition rate of In2 in the solution and in the nanocomposite as well; this rate depends on the photoinitiator/AuNPs ratio, being higher for higher this ratio.

Scheme of In2 decomposition mechanism is well investigated and presented in different research works as it is shown in Figure 4 [33]. The interaction between the In2 photoinitiator and AuNPs was studied also by FTIR spectroscopy. Dry residues of pure SIn and SInAu2 were investigated before and after UV irradiation. Fig. 8 compares FTIR spectra of the dry

residues of toluene solutions of pure SIn and SInAu2 before and after irradiation. The addition of AuNPs to the untreated material results in weak conformational changes, as it can be seen from the differences between the spectra.

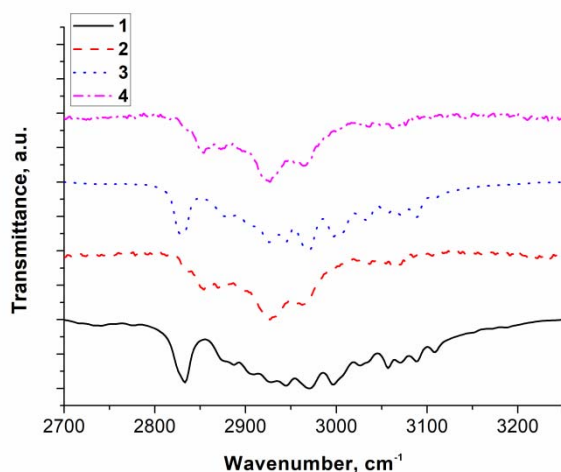


Figure 8. FTIR spectra of a dry residue of SIn and SInAu before (bef) and after (aft) irradiation by 325 nm: 1- SIn bef; 2 – SIn aft; 3- SInAu2 bef; 4 – SInAu2 aft.

For example, the intensity ratios of aromatic sp^2CH peaks change in the $3040 - 3100 \text{ cm}^{-1}$ spectral region. In the $2850 - 3200 \text{ cm}^{-1}$ spectral range a more subtle structure of the spectrum appears. After irradiation, the peak at 2830 cm^{-1} , related to the methyl vibrations of the molecule, disappears as well as most of the aromatic sp^2CH peaks above 3000 cm^{-1} . These changes indicate the disappearance of the phenyl ring oscillations and their transformation into less complex C – H bonds.

All these spectral changes imply the presence of weak interaction of the phenyl ring with AuNPs, resulting in an unstable complex. Thus, weak interaction between In2 photoinitiator and AuNPs occurs, followed by an unstable complex both in the solution and in the nanocomposite. However, this weak complex leads to stabilization of the In2 and reduces the In2 decomposition rate under irradiation by 325 nm light. Also, it is important to note that AuNPs do not absorb light at 325 nm resonantly. This is the reason why there is no destabilizing effect of localized plasmons during irradiation which has been seen during 532nm irradiation of nanocomposites with Irg784.

It was shown earlier [27,28] that adding AuNPs to the polymer nanocomposite influences on the photopolymerization process (on the degree of polymerization as well as on the rate of the refractive index change at polymerization) and so on the parameters of

holographic recording (diffraction efficiency and amplitude of created surface structure) as well. The character and the feature of this influence were dependent on the composition, type of the photoinitiator and irradiation parameters as well. Continuing this investigation we showed by our experiments that AuNPs have an influence on the decomposition rate of photoinitiator during photopolymerization process for the investigated monomers (UDMA+IDA). In one case AuNPs form a stable complex with the photoinitiator - Irg784. The photoinitiator decomposition rate increases in this nanocomposite and this should change the polymerization rate. Thus, the addition of AuNPs to this nanocomposite reduced the modulation parameters (and so the resulting diffraction efficiency) of the created PhC. It was shown in our previous paper, that in nanocomposite based on UDMA and IDA monomers and Irg784, adding AuNPs decreased the amplitude of the created surface structures and their diffraction efficiency as well [29]. While in the other case AuNPs form an unstable complex with In2 photoinitiator, which decreases the decomposition rate and the rate of photopolymerization [27, 28]. As a result, this process enhanced the parameters of the PhC, created due to the polymerization with longer mass transport. It was shown in our other papers, that in nanocomposite based on UDMA and IDA monomers and In2, adding AuNPs decreased the rate of photopolymerization, while the amplitude of the created surface structures and their diffraction efficiency was increased [27,28]. As matter of fact, AuNPs influence the process of holographic recording and also the parameters of created PhC. The nature of the influence depends on the composition, monomers, photoinitiators, and nanoparticles. So by these elements, the parameters of the surface structures could be controlled.

As the decomposition of the photoinitiator during the photopolymerization process is only one element which could influence on the optical recording so on the parameters of the created surface structures, other elements should be investigated to clear the complex mechanism of this process. In the next step, the influence of AuNPs on chain growth should be analyzed during the photopolymerization process, which possibly influences the material transport in periodically illuminated nanocomposites and so the parameters of created photonic elements.

Conclusion

In this work, we examined the effect of gold nanoparticles on the decomposition rate of photoinitiators in different media: in polymer nanocomposites and in toluene solution

under the action of radiation within and out of the spectral region of the AuNPs plasmon resonance. It was established that AuNPs influence on the decomposition rate of photoinitiator during photopolymerization process, thus can essentially change the polymerization of the nanocomposite. The observed changes in the decomposition rates were explained by complex formation between the photoinitiator and gold nanoparticles that results in stable structures with Irg784 and unstable ones with an In2 photoinitiator. FTIR spectroscopic studies supported this assumption and confirmed the transformation of the photoinitiator structure in the presence of AuNPs and the formation of complexes. So adding AuNPs to the polymer nanocomposite influences on the polymerization process (on the rate and degree of photopolymerization, on the mass transport in the non-uniformly irradiated films, redistribution of components during polymerization) which in turn determine the rate and degree of the local volume and refractive index change at polymerization. This way the parameters of holographic recording (phase modulation, the amplitude of created surface structures, the diffraction efficiency of the recorded photonic elements) can be controlled.

Acknowledgment

The authors acknowledge the financial support by the grant GINOP-2.3.2-15-2016-00041 and VEKOP-2.3.2-16-2016-00011. M.V. is grateful for the support of the Bolyai János Scholarship of the Hungarian Academy of Sciences.

References:

1. Song, S.W.; Jeong, Y.; Kwon S. Photocurable Polymer Nanocomposites for Magnetic, Optical, and Biological Applications, *IEEE Journal of Selected Topics in Quantum Electronics*, **2015**, 21, 4.
2. Lengm J.; Lau A. K. Multifunctional Polymer Nanocomposites, *CRC Press*, **2010**.
3. Suzuki, N.; Tomita, Y.; Kojima, T. Holographic recording in TiO₂ nanoparticle-dispersed methacrylate photopolymer films, *Appl. Phys. Lett.*, **2002**, 81, 4121-4123.

4. Suzuki, N.; Tomita, Y. Silica-nanoparticle-dispersed methacrylate photopolymers with net diffraction efficiency near 100%, *Applied Optics*, **2004**, 43, 2125-2129.
5. Suzuki, N.; Tomita, Y.; Ohmori, K.; Hidaka, M.; Chikama, K. Highly transparent ZrO₂ nanoparticle-dispersed acrylate photopolymers for volume holographic recording, *Optics Express*, **2006**, 14, 12712-12719.
6. Tomita, Y.; Furushima, K. Organic nanoparticle (hyperbranched polymer)-dispersed photopolymers for volume holographic storage, *Appl. Phys. Lett.*, **2006**, 88, 10.1063/1.2175485
7. Liu, X.; Tomita, Y.; Oshima, J.; Chikama, K.; Matsubara, K.; Nakashima, T.; Kawai, T. Holographic assembly of semiconductor CdSe quantum dots in polymer for volume Bragg grating structures with diffraction efficiency near 100%, *Appl. Phys. Lett.*, **2009**, 95, 261109.
8. Tomita, Y.; Hata, E.; Momose, K.; Takayama, S.; Liu, X.; Chikama, K.; Klepp, J.; Pruner, C.; Fally, M. Photopolymerizable nanocomposite photonic materials and their holographic applications in light and neutron optics, *J Mod Opt.*, **2016**, 63, S1–S31.
9. Smirnova, T.; Sakhno, O.; Lozenko S. The effect of structural-kinetic features of hologram formation on holographic properties of photopolymers, *Semiconductor Physics, Quantum Electronics & Optoelectronics*, **2004**, 7, 326-331.
10. Daniel, M.C.; Astruc, D. Gold nanoparticles: assembly, supramolecular chemistry, quantum-size-related properties, and applications toward biology, catalysis, and nanotechnology. *Chem. Rev.* **2004**, 104, 293-346.
11. Krasteva, N.; Krustev, R.; Yasuda, A.; Vossmeier, T. Vapor sorption in self-assembled gold nanoparticle/dendrimer films studied by specular neutron reflectometry. *Langmuir*. **2003**, 19, 7754–7760.
12. Juhl, A.T.; Busbee, J. D.; Koval, J. J.; Natarajan, L. V.; Tondiglia, V. P.; Vaia, R. A.; Bunning, T. J.; Braun, P. V. Holographically directed assembly of polymer nanocomposites. *ACS Nano*. **2010**, 4, 5953–5961.
13. Brust, M.; Kiely, C. J. Some recent advances in nanostructure preparation from gold and silver particles: a short topical review. *Colloids Surf., A* **2002**, 202, 175-186.
14. Templeton, A. C.; Wuelfing, W. P.; Murray R. W. Monolayer-protected cluster molecules. *Acc. Chem. Res.* **2000**, 33, 27-36.
15. Fedlheim, D. L.; Foss, C. A. Metal nanoparticles: synthesis, characterization, and applications. CRC Press, **2001**.
16. Tian, Y.; Tatsuma, T. Mechanisms and applications of plasmon-induced charge separation at TiO₂ films loaded with gold nanoparticles. *J. Am. Chem. Soc.* **2005**, 127, 7632-7637.

17. Tian, Y.; Notsu, H.; Tatsuma, T. Visible-light-induced patterning of Au–and Ag–TiO₂ nanocomposite film surfaces on the basis of plasmon photoelectrochemistry. *Photochem. Photobiol. Sci.* **2005**, *4*, 598-601.
18. Zhang, J.; Whitesell, J. K.; Fox, M. A. Photoreactivity of self-assembled monolayers of azobenzene or stilbene derivatives capped on colloidal gold clusters. *Chem. Mater.* **2001**, *13*, 2323-2331.
19. Ipe B. I.; Thomas, K. G.; Barazzouk, S.; Hotchandani, S.; Kamat, P. V. Photoinduced charge separation in a fluorophore-gold nanoassembly. *J. Phys. Chem. B* **2002**, *106*, 18-21.
20. Nakashima, T.; Sakashita, M.; Nonoguchi, Y.; Kawai, T. Sensitized photopolymerization of an ionic liquid-based monomer by using CdTe nanocrystals. *Macromolecules.* **2007**, *40*, 6540-6544.
21. Anyaogu, K. C.; Cai, X.; Neckers, D. C. Gold nanoparticle photosensitized radical photopolymerization. *Photochem. Photobiol. Sci.* **2008**, *7*, 1469-1472.
22. Anyaogu, K. C.; Cai, X.; Neckers, D. C. Gold nanoparticle photopolymerization of acrylates. *Macromolecules.* **2008**, *41*, 9000-9003.
23. Collins, G.; Armstrong, E.; McNulty, D.; O’Hanlon, S.; Geaney, H.; O’Dwyer, C. 2D and 3D photonic crystal materials for photocatalysis and electrochemical energy storage and conversion, *Science and Technology of Advanced Materials*, **2016**, 563-582.
24. Troia, B.; Paolicelli, A.; De Leonardis, F.; M. N. Passaro, V. Photonic Crystals for Optical Sensing: A Review, *Advances in Photonic Crystals*, InTech, **2013**.
25. Burunkova, J.A; Denisiuk, I. Yu.; Zhuk, D. Zh.; Daroczi, L.; Csik, A.; Csarnovics, I.; Kokenyesi, S. Fabrication and properties of luminescence polymer composites with erbium/ytterbium oxides and gold nanoparticles. *Beilstein J. Nanotechnol.* **2016**, *7*, 630–636.
26. Sakhno, O. V.; Goldenberg, L. M; Stumpe, J.; Smirnova, T. N. Surface modified ZrO₂ and TiO₂ nanoparticles embedded in organic photopolymers for highly effective and UV-stable volume holograms. *Nanotechnology.* **2007**, *18*, 105704.
27. Burunkova, J.; Denisiuk, I.; Vorzobova, N.; Daroczi, L.; Hegedus, Cs.; Charnovych, S.; Kokenyesi, S. Fabrication and Characterization of Gold/Acrylic Polymer Nanocomposites. *Eur. Polym. J.* **2013**, *49*, 3072–3077.
28. Burunkova, J.A; Kokenyesi, S.; Csarnovics, I.; Bonyár, A.; Veres, M.; Csik, A. Influence of gold nanoparticles on the photo-polymerization processes and structure in acrylate nanocomposites. *European Polymer Journal*, **2015**, *64*, 189–195.
29. Zhuk, D. Zh.; Burunkova, J.A; Denisiuk, I. Yu.; Mirosnichenko, G. P.; Csarnovics, I.; Toth, D.; Bonyar, A.; Veres, M.; Kokenyesi, S. Peculiarities of Photonic Crystal Recording in Functional Polymer Nanocomposites by Multibeam Interference Holography, *Polymer*, **2017**, *112*, 136-143.
30. Sabol, D.; Gleeson, M.R.; Liu, S.; Sheridan, J.T., Photoinitiation study of Irgacure 784 in an epoxy resin photopolymer, *J. Appl. Phys.* **2010**, *107*, 053113.

31. Lin, S. H.; Hsiao, Y. N.; Hsu, K. Y. Preparation and characterization of Irgacure 784 doped photopolymers for holographic data storage at 532 nm. *J. Opt. A: Pure Appl. Opt.* **2009**, *11*, 024012.
32. Sabol, D.; Gleeson, M. R.; Liu, S.; Sheridan, J. T. Photoinitiation study of Irgacure 784 in an epoxy resin photopolymer, *Journal of Applied Physics*, **2010**, *107*, 053113.
33. Fischer, H.; Baer, R.; Hany, R.; Verhoolen, I.; Walbiner, M. 2,2-Dimethoxy-2-phenylacetophenone: Photochemistry and Free Radical Photo-fragmentation. *J. Chem. Soc. Perkin trans.* **1990**, *2*, 787- 798.
34. Veres, M.; Koos, M.; Pocsik, I. IR study of the formation process of polymeric hydrogenated amorphous carbon film. *Diamond Relat. Mater.* **2002**, *11*, 1110–1114.